ELSEVIER

Journal of Atmospheric and Solar-Terrestrial Physics 67 (2005) 1761–1766

Journal of ATMOSPHERIC AND SOLAR-TERRESTRIAL PHYSICS

www.elsevier.com/locate/jastp

Magnetic clouds: A statistical study of magnetic helicity

A.M. Gulisano[a,*], S. Dasso[a,b], C.H. Mandrini[a], P. Démoulin[c]

[a]*Instituto de Astronomía y Física del Espacio (IAFE), CONICET-UBA, Ciudad Universitaria, CC 67-Suc. 28, 1428 Buenos Aires, Argentina*

[b]*Departamento de Física, Facultad de Ciencias Exactas y Naturales, Universidad de Buenos Aires, 1428 Buenos Aires, Argentina*

[c]*Observatoire de Paris, LESIA, UMR 8109 (CNRS), F-92192, Meudon Cedex, France*

Available online 29 August 2005

Abstract

We select a set of 20 magnetic clouds (MCs) observed by the spacecraft Wind and reconstruct their local magnetic structure from in situ observations under different models. In particular, we quantify their relative magnetic helicity per unit length (H_r/L) under the assumption of a cylindrical geometry. We investigate how model-dependent are the results using four models (two force-free and two non-force-free) with a significantly different twist distribution in their magnetic field: (a) a linear force-free field, (b) a uniformly twisted field, (c) a non-force-free field with constant current (**J**) and (d) a non-force-free field with an azimuthal component of **J** depending linearly on the radius and with a constant axial component of **J**. We find that the dispersion of the mean H_r/L for the 20 MCs is one order of magnitude larger than the dispersion of the H_r/L value using different models for a given event. In this sense, magnetic helicity per unit length is a well-determined magnitude considering these four models.

Keywords: Interplanetary medium; Solar wind; Magnetic clouds; Space physics; Magnetohydrodynamics; Magnetic helicity

1. Introduction

Magnetic clouds (MCs) are the interplanetary manifestation of magnetized plasma ejected from the solar surface. Despite MCs have been observed for more than 20 years, the details of their magnetic configuration and typical values for their magnetohydrodynamic (MHD) magnitudes are not yet well known. This is mainly because the spacecraft can only obtain in situ measurements along a linear cut and we have to trust in fittings to models to deduce their global structure.

One important MHD quantity in MCs is the magnetic helicity (MH). When the source of the MC is ejected from the solar surface, the magnetized plasma carries a significant amount of MH that is transported into the interplanetary space by the MC. MH is almost conserved in plasmas with low resistivity (as the solar corona and the heliosphere). Thus, it is important to quantify global magnitudes of MCs, such as their MH to compare them with their solar counterparts (see e.g. Nindos et al., 2003; Mandrini et al., 2005; Luoni et al., 2005).

MCs can be locally modeled in cylindrical geometry under four different approaches: (a) a linear force-free field model, as was first suggested by Goldstein (1983), (b) a uniformly twisted field (Farrugia et al., 1999), (c) a non-force-free field with constant current (Hidalgo et al., 2000), and (d) a non-force-free field with an azimuthal component of the current (**J**) depending linearly on the radius and a constant axial component of **J** (Cid et al.,

*Corresponding author. Tel.: +54 11 4783 2642; fax: +54 11 4786 8114.

E-mail address: agulisano@iafe.uba.ar (A.M. Gulisano).

1364-6826/$ - see front matter © 2005 Elsevier Ltd. All rights reserved.
doi:10.1016/j.jastp.2005.02.026

2002). All these models are physically different and it is not clear how close the real configuration of an MC is from each one of them.

Several statistical works have analyzed the MCs properties using cylindrical models (e.g., Lepping et al., 1990; Zhao et al., 2001). From the results of these two studies, and assuming the Lundquist's model, Green et al. (2002) and van Driel-Gesztelyi et al. (2003) estimated that the average MH in clouds was $\sim 2 \times 10^{42}\,\mathrm{Mx}^2$. However, no statistical works quantifying MH with different models have yet been done.

In this work, we study a set of 20 MCs observed by the spacecraft Wind and reconstruct their local magnetic structure from in situ observations. We quantify their relative MH per unit length (H_r/L) using the four cylindrical models mentioned above. We find that its relative variation range (when considering the four different models for each event) turns out to be of ~10% averaging the 20 events. Then, H_r/L can be considered an almost model-independent magnitude. This kind of analysis is a good starting point to carry out future studies connecting solar events with their associated interplanetary manifestations.

In Section 2, we describe the analyzed data and the method used to process them. The four models mentioned above, a comparison of the physical parameters derived from them, and the obtained values of the helicity per unit length, are presented in Section 3. Finally, in Section 4, we summarize our conclusions.

2. Data analysis

We select a set of MCs observed by the spacecraft Wind from 22 August 1995 to 7 November 1997 (during a solar minimum), according to the list given in the following web page: http://lepmfi.gsfc.nasa.gov/mfi/mag_cloud_pub1.

We analyze the magnetic data from the Magnetic Field Instrument (Lepping et al., 1995), aboard the spacecraft Wind, downloaded from http://cdaweb.gsfc.nasa.gov/cdaweb/istp_public/, in Geocentric Solar Ecliptic (GSE) coordinates with a temporal cadence of 3 s. Since our aim is to better understand the large-scale magnetic structure of the clouds, we smoothed the data to obtain 100 averaged points for each cloud.

In our approach, the orientation of the axis of the cloud is determined for every event using a minimum variance (MV) analysis, as discussed in Bothmer and Schwenn (1998) and Dasso et al. (2003b). From this analysis, we obtain: (a) the latitude angle (θ) between the cloud axis (defined in such a way that $\theta > 0$ when the axial component of the magnetic field at the cloud axis points northward) and the ecliptic plane and (b) the longitude angle (φ) between the projection of the cloud axis on the ecliptic plane and the Earth–Sun direction ($\mathbf{X}_{\mathrm{GSE}}$), measured counterclockwise. Thus, from this cloud orientation we find the radius (R), using the cloud mean speed and the time interval of Wind observations. We can also determine the sign of the helicity (defined as positive for a right-hand helix) from the global behavior of the observed field components. The list of the start and end times, θ, φ, R and the helicity sign are given in Table 1 for the complete set of analyzed clouds.

Taking into account the MV orientation of the cloud local axis (θ, φ), we rotate the GSE components of the field obtaining the new components in the cloud frame. In this frame, $\mathbf{X}_{\mathrm{cloud}}$ corresponds to the cylindrical radial direction ($\mathbf{r}$) in the ideal case of the spacecraft crossing the axis of the cloud (null impact parameter) as it leaves the structure, $\mathbf{Z}_{\mathrm{cloud}}$ is parallel to the axis of the cylinder (sign such that $B_{z,\mathrm{cloud}}$ is positive at the cloud axis) and $\mathbf{Y}_{\mathrm{cloud}}$ completes a right-handed reference system.

Fig. 1 shows the three 'cloud' components of the field for event #8 (see Table 1). Dashed lines mark the beginning and the end of the observed event. It can be clearly seen that the fluctuations in $B_{x,\mathrm{cloud}}$ (upper panel) are low; we also observe the large variation in $B_{y,\mathrm{cloud}}$ (central panel) that changes its sign as the spacecraft passes near the center of the cloud and, finally, (lower panel) that $B_{z,\mathrm{cloud}}$ is maximum at the center of the cloud and close to zero in its two boundaries (with an intermediate variance).

3. MH per unit length for the four cylindrical models

We analyze the observations assuming four different models with cylindrical symmetry in the 2D cut (slice) of the magnetic field configuration, corresponding to the intersection of the spacecraft trajectory with the MC. In particular, the observations are used to fit the free parameters of the four models described below:

(1) The cylindrical linear force-free field, known as the Lundquist's model (L) (Lundquist, 1950), is given by $\mathbf{B} = B_0[J_1(\alpha r)\boldsymbol{\phi} + J_0(\alpha r)\mathbf{z}]$, with J_n the Bessel function of the first kind of order n, B_0 is the strength of the field, and α is a constant. The magnetic field lines have a different twist for different radial distances from the cloud axis in this configuration. The twist per unit length, $\tau = \mathrm{d}\phi/\mathrm{d}z = B_\phi/(rB_z)$, results in $\tau(r) = J_1(\alpha r)/rJ_0(\alpha r)$, being the twist at the axis $\tau_0 = \tau(0) = \alpha/2$. A relative MH, gauge-independent, can be defined in helical structures (see, e.g., Dasso et al., 2003a) and the relative helicity (H_r) per unit length can be expressed in this model as (Dasso et al., 2003b)

$$H_r/L = 4\pi B_0^2 \alpha^{-1} \int_0^R J_1^2(\alpha r) r\,\mathrm{d}r.$$

Table 1
List of studied magnetic clouds

Event	Start	End	θ (deg)	φ (deg)	R (10^{-2} AU)	Helicity sign
#1	22 Aug. 1995, 22:00	23 Aug. 1995, 19:00	−22.7	271.2	9.1	+
#2	18 Oct. 1995, 19:00	20 Oct. 1995, 00:00	−13.7	286.9	13.7	+
#3	16 Dec. 1995, 05:00	16 Dec. 1995, 22:00	−12.1	51.2	6.5	−
#4	27 May 1996, 15:00	29 May 1996, 07:00	−2.3	132.2	13.2	−
#5	01 Jul. 1996, 17:00	02 Jul. 1996, 09:00	3.0	105.1	6.5	−
#6	07 Aug. 1996, 13:00	08 Aug. 1996, 10:00	−64.6	292.4	8.6	+
#7	24 Dec. 1996, 03:00	25 Dec. 1996, 10:00	50.9	80.3	13.0	+
#8	10 Jan. 1997, 05:00	11 Jan. 1997, 02:00	−18.1	244.4	10.1	+
#9	21 Apr. 1997, 15:00	23 Apr. 1997, 07:00	16.6	333.3	8.9	+
#10	15 May 1997, 09:00	16 May 1997, 01:00	−15.9	111.9	8.4	−
#11	16 May 1997, 07:00	16 May 1997, 14:00	−30.3	303.0	3.6	−
#12	09 Jun. 1997, 02:00	09 Jun. 1997, 23:00	−17.8	238.1	8.2	+
#13	19 Jun. 1997, 05:06	19 Jun. 1997, 17:54	−61.0	216.8	4.7	+
#14	15 Jul. 1997, 06:00	16 Jul. 1997, 01:00	−63.8	124.6	8.2	−
#15	03 Aug. 1997, 14:00	04 Aug. 1997, 01:00	−11.5	31.5	3.2	−
#16	18 Sep. 1997, 00:00	20 Sep. 1997, 12:00	60.1	203.5	20.5	+
#17	21 Sep. 1997, 22:00	22 Sep. 1997, 18:00	72.1	163.5	9.9	−
#18	01 Oct. 1997, 16:00	02 Oct. 1997, 23:00	35.3	127.8	14.8	−
#19	10 Oct. 1997, 23:00	12 Oct. 1997, 00:00	−15.0	256.9	12.0	+
#20	07 Nov. 1997, 05:48	08 Nov. 1997, 04:18	−5.2	225.7	8.4	+

The start and end times, latitude (θ) and longitude (φ) of the cloud axis, radius (R) of the flux tube, and the helicity sign, are shown.

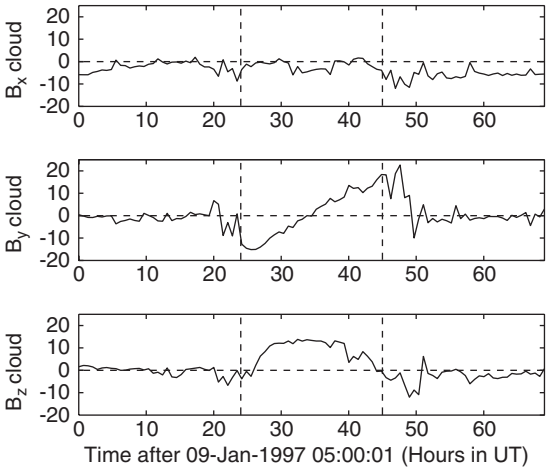

Fig. 1. Magnetic field components (nT) in the frame of the cloud for event #8 (see text for details of cloud coordinates). The beginning and the end of the event are marked with vertical dashed lines.

(2) The cylindrical uniformly twisted field, known as the Gold–Hoyle's model (GH) (Gold and Hoyle, 1960), is given by $\mathbf{B} = B_0 br/(1 + b^2r^2)\boldsymbol{\phi} + B_0/(1 + b^2r^2)\mathbf{z}$. In this model, the amount by which a given line is twisted is independent of r: $\tau(r) = \tau_0 = b$. The relative MH per unit length is (Dasso et al., 2003a) $H_r/L = (\pi B_0^2/2b^3)[\ln(1 + b^2R^2)]^2$.

(3) A non-force-free field with constant current, the Hidalgo's et al. model (H) (Hidalgo et al., 2000), has been used to model MCs. This model assumes a constant current density in the cloud, such as $\mathbf{J} = J_\phi\boldsymbol{\phi} + J_z\mathbf{z}$, with J_ϕ and J_z constants. The magnetic field of this configuration is $\mathbf{B} = B_0\tau_0 r\boldsymbol{\phi} + B_0(1 - r/R)\mathbf{z}$, where $B_0 = \mu_0 J_\phi R$ is the maximum field at the center of the cloud and $\tau_0 = J_z/(2RJ_\phi)$. The twist distribution in this model turns out to be $\tau(r) = \tau_0/(1 - r/R)$. The relative MH per unit length can be written as: $H_r/L = 7\pi B_0^2 R^4\tau_0/30$ (Dasso et al., 2003b).

(4) A non-force-free field with an azimuthal component of the current, depending linearly on the radius, and a constant axial component of $\mathbf{J}$, the Cid's et al. model (C) (Cid et al., 2002) has been also used to describe the magnetic structure of MCs. The magnetic field in this model is $\mathbf{B} = B_0\tau_0 r\boldsymbol{\phi} + B_0(1 - r^2/R^2)\mathbf{z}$, the axial twist $\tau_0 = J_z/B_0$) and the relative MH per unit length $H_r/L = \pi B_0^2 R^4\tau_0/3$ (Dasso et al., 2005).

We determine the free parameters (B_0 and τ_0) of the magnetic field, in the cloud frame and for each of the four models, using the standard non-linear least-square fitting Levenberg–Marquardt routine (Press et al., 1992). Then, from the fitted parameters, we compute the MH for each event and each model. Figs. 2 and 3 show an example of the fitted results, where the components

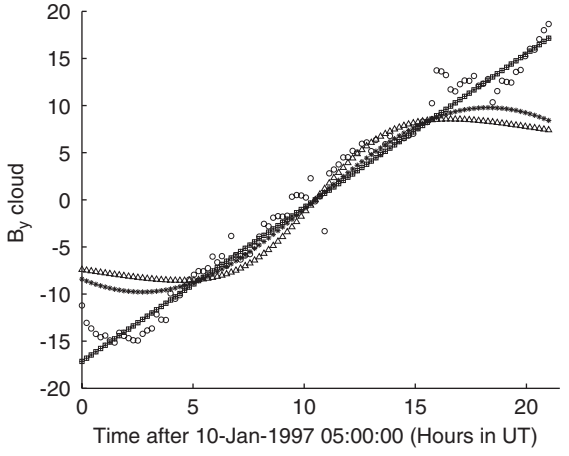

Fig. 2. $B_{y,\mathrm{cloud}}$ component of the magnetic field (nT). (○) show the observed field. (*,△,□,+) Models L, GH, H, and C, respectively. The curves for H and C models are overplotted.

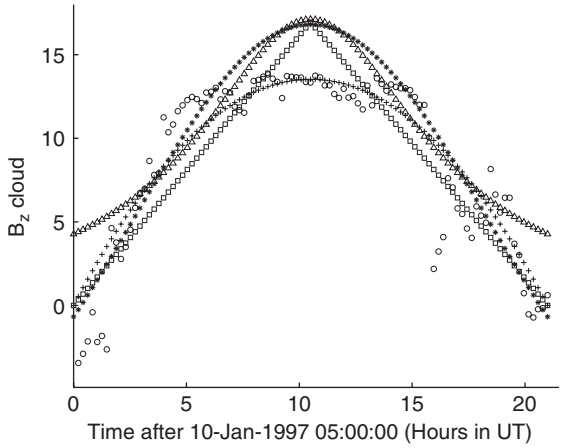

Fig. 3. Idem Fig. 2, but showing $B_{z,\mathrm{cloud}}$.

$B_{y,\mathrm{cloud}}$ and $B_{z,\mathrm{cloud}}$ can be seen, respectively, together with the curves obtained from the four models. Close to the cloud center, $B_{z,\mathrm{cloud}}$ is overestimated by models L, GH, and H; while model GH also overestimates the two field components near the cloud boundaries. The absolute value of $B_{y,\mathrm{cloud}}$ is underestimated by the two force-free models (L and GH) near the cloud boundaries. According to these figures, and also to the computed square difference between the observations and the modeled field components, model C gives the best fit for this event. From a visual inspection and from the square difference, model C gives the best fit in eight of the 20 clouds analyzed in this paper, model GH in 5/20, L in 4/20, and H in 3/20.

Fig. 4 shows the fitted values of B_0 for every event in Table 1. It shows that, in general, model C tends to give lower values of B_0 (13 of the 20 clouds), while model H gives larger values (also in 13 of the 20 clouds). The dispersion in B_0 when the two force-free models (L and GH) are used is much lower than for models H and C. We also note that the variation of B_0 for different events is generally larger than the dispersion of B_0 for a given event when the four models are considered.

The absolute values of the fitted axial twist of the magnetic field lines ($|\tau_0|$) are shown in Fig. 5. In this figure, model GH (shown with triangles and a dot-dashed line) gives the larger values of $|\tau_0|$ for all the analyzed clouds and model H (squares and dashed line) the lower values. The axial twist obtained from models L and C are not well ordered.

The absolute value of the relative MH per unit length, $|H_r/L|$, is shown in Fig. 6 for the different models and events. In cylindrical flux tubes, and for a given central magnetic flux across a surface perpendicular to the cloud axis, larger values of the azimuthal field (proportional to τ)

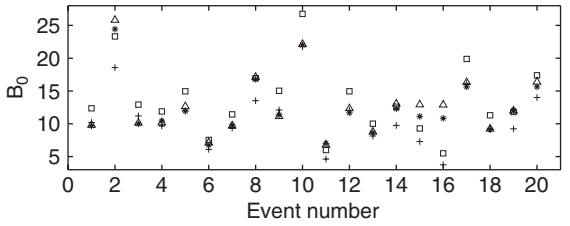

Fig. 4. Maximum field at the cloud axis, B_0 in nT, fitted from the four different models for the 20 analyzed events. (*,△,□,+) Models L, GH, H, and C, respectively.

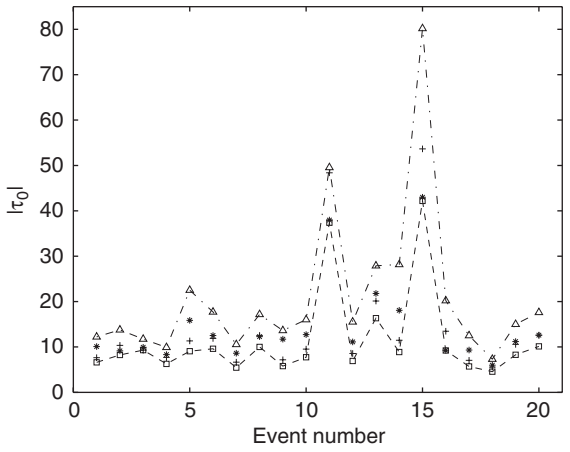

Fig. 5. Absolute value of the axial twist of the magnetic field lines per unit length ($|\tau_0|$ in AU^{-1}), computed from the four models and for the 20 clouds. Each symbol corresponds to each model as in Fig. 4. Twist from model GH is indicated also with dot–dashed lines and gives the larger values. Model H is also marked with dashed lines to stress that it corresponds to the lowest values.

in the tube periphery correspond to a larger value of the MH. In model GH, $\tau_{GH}(r)$ is constant, but $\tau(r)$ is a monotonic increasing function for models L, H, and C, being $\tau_{GH}(r{\sim}R)$ much lower than for the rest of the models. Thus, we expect a trend to lower values of $|H_r/L|$ in model GH. The obtained lower values for $|H_r/L|$ correspond to model GH (13 clouds) and model H (7 clouds). Model C gives the larger values for $|H_r/L|$ in 13 clouds and model L in the other 7 events.

For a given event (^{j}) we compute the average of $|H_r/L|$ over the four models ($_i$), as

$$H^j_{\text{mean}} = \frac{1}{4}\sum_{i=1}^{4} |H_r/L|^j_i,$$

where 'mean' stands for the average using the four models.

Thus, the average dispersion among models can be calculated as follows:

$$\langle \sigma_{H_{\text{models}}} \rangle = \frac{1}{20}\sum_{j=1}^{20} \sqrt{\tfrac{1}{4}\sum_{i=1}^{4} \left(|H_r/L|^j_i - H^j_{\text{mean}}\right)^2},$$

where $\langle \ldots \rangle$ means the average among events.

On the other hand, the average of the relative variation range of $|H_r/L|$ is given by

$$\langle \sigma_{\text{relative}} \rangle = \left\langle \frac{\sigma_{H_{\text{models}}}}{H_{\text{mean}}} \right\rangle = \frac{1}{20}\sum_{j=1}^{20} \left(\sqrt{\frac{1}{4}\sum_{i=1}^{4} (|H_r/L|^j_i - H^j_{\text{mean}})^2} \Big/ H^j_{\text{mean}} \right)$$

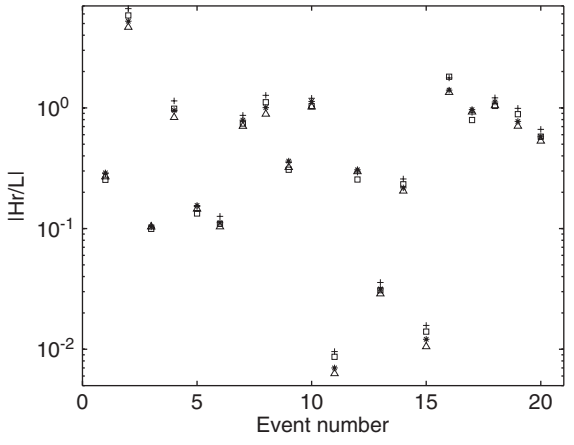

Fig. 6. Absolute value of relative magnetic helicity per unit length, $|H_r/L|$, in units of $10^{42}\,\text{Mx}^2/\text{AU}$, for all the studied events. Symbols (as in Fig. 4) show $|H_r/L|$ computed from the four models.

and the dispersion of H_{mean} among events is given as:

$$\sigma_{H_{\text{events}}} = \sqrt{\frac{1}{20}\sum_{j=1}^{20}\left(H^j_{\text{mean}} - \left(\frac{1}{20}\sum_{j=1}^{20} H^j_{\text{mean}} \right)^2 \right)}.$$

Fig. 6 shows that the dispersion of the $|H_r/L|$ values when changing from model ($\langle \sigma_{H_{\text{models}}} \rangle {\sim} 10^{41}\,\text{Mx}^2/\text{AU}$) is much lower than the dispersion when the events are changed ($\sigma_{H_{\text{events}}} {\sim} 10^{42}\,\text{Mx}^2/\text{AU}$).

The average of the relative variation range of $|H_r/L|$ is $\langle \sigma_{\text{relative}} \rangle = 0.1$; thus, in this sense, H_r/L is a magnitude that depends little on the analized models.

4. Conclusions

To improve the knowledge of the physical characteristics of MCs and of their solar source regions, the quantification of global magnitudes is needed. In the last few years, several works (Démoulin et al., 2002; Green et al., 2002; Nindos et al., 2003; Mandrini et al., 2005; Luoni et al., 2005) have computed the MH variation in active regions (for particular events or global budget) and have compared it to the helicity in MCs. However, no study of the helicity content in a large set of MCs using different models has yet been done.

Even though in the interplanetary medium the observations are done in situ, these data are insufficient to determine the real 3D magnetic configuration of MCs. Therefore, we explored here four different models to represent the MCs structure in their local cross-section and we computed their MH per unit length along the cloud (H_r/L).

From our statistical study of 20 MCs, we found that the axial twist ($|\tau_0|$) resulted lower for model H, while it was larger for model GH, in all cases. We found a slight trend to obtain lower values of $|H_r/L|$ from model GH, and larger values from model C. However, despite the important variations in the distribution of the twist assumed by the different models, we found that the dispersion of the obtained values of H_r/L, using different models for a given cloud, is one order of magnitude lower than the dispersion of H_r/L for different events. In this sense, H_r/L is almost independent from the model used.

Acknowledgments

We thank the referees for useful comments that helped to improve our paper. This research has made use of NASA's Space Physics Data Facility (SPDF). This work was partially supported by the Argentinean grants: UBACyT X329, and PICTs 12187 and 14163 (ANPCyT). S.D. acknowledges Observatoire de Paris,

Meudon, for visiting financial support. P.D. and C.H.M. thank CONICET (Argentina) and CNRS (France) for their cooperative science project. S.D. and C.H.M. are members of the Carrera del Investigador Científico, CONICET.

References

Bothmer, V., Schwenn, 1998. The structure and origin of magnetic clouds in the solar wind. Annales Geophysicae 16, 1–24.

Cid, C., Hidalgo, M.A., Nieves-Chinchilla, T., Sequeiros, J., Viñas, A.F., 2002. Plasma and magnetic field inside magnetic clouds: a global study. Solar Physics 207, 187–198.

Dasso, S., Mandrini, C.H., Démoulin, P., 2003a. The magnetic helicity of an interplanetary hot flux rope. AIP Conference Proceedings: Solar Wind Ten 679, 786–789.

Dasso, S., Mandrini, C.H., Démoulin, P., Farrugia, C.J., 2003b. Magnetic helicity analysis of an interplanetary twisted flux tube. Journal of Geophysical Research (Space Physics) 108, 1362.

Dasso, S., Mandrini, C.H., Démoulin, P., Luoni, M.L., Gulisano, A.M., 2005. Large scale MHD properties of interplanetary magnetic clouds. Advances in Space Research 35, 711–724.

Démoulin, P., Mandrini, C.H., van Driel-Gesztelyi, L., Thompson, B.J., Plunkett, S., et al., 2002. What is the source of magnetic helicity shed by CMEs? The long-term helicity budget of AR 7978. Astronomy and Astrophysics 382, 650–665.

Farrugia, C.J., Janoo, L.A., Torbert, R.B., Quinn, J.M., Ogilvie, K.W., et al., 1999. A uniform-twist magnetic flux rope in the solar wind. In: Habbal, S.R., et al. (Eds.), Solar Wind Nine AIP Conference Proceedings 471, pp. 745–748.

Gold, T., Hoyle, F., 1960. On the origin of solar flares. Monthly Notices of the Royal Astronomical Society 120, 89–105.

Goldstein, H., 1983. On the field configuration in magnetic clouds, in Solar Wind 5, NASA Conference Publication CP-2280, p. 731.

Green, L.M., López Fuentes, M.C., Mandrini, C.H., Démoulin, P., van Driel-Gesztelzyi, L., Culhane, J.L., 2002. The magnetic helicity budget of a CME-Prolific active region. Solar Physics 208, 43–68.

Hidalgo, M.A., Cid, C., Medina, J., Viñas, A.F., 2000. A new model for the topology of magnetic clouds in the solar wind. Solar Physics 194, 165–174.

Lepping, R.P., Burlaga, L.F., Jones, J.A., 1990. Magnetic field structure of interplanetary magnetic clouds at 1 AU. Journal of Geophysical Research (Space Physics) 102, 11957–11965.

Lepping, R.P., Acuña, M., Burlaga, L., Farrell, W., Slavin, J., et al., 1995. The WIND magnetic field investigation. Space Science Reviews 71, 207.

Lundquist, S., 1950. Magnetohydrostatic fields. Arkiv for Fysik 2, 361–365.

Luoni, M.L., Mandrini, C.H., Dasso, S., van Driel-Gesztelyi, L., Démoulin, P., 2005. Tracing magnetic helicity from the solar Corona to the interplanetary space. JASTP in press.

Mandrini, C.H., Pohjolainen, S., Dasso, S., Green, L.M., Démoulin, P., et al., 2005. Interplanetary flux rope ejected from an X-ray bright point: the smallest magnetic cloud source region ever observed. Astronomy & Astrophysics 434, 725–740.

Nindos, A., Zhang, J., Zhang, H., 2003. The magnetic helicity budget of solar active regions and coronal mass ejections. Astrophysics Journal 594, 1033–1048.

Press, W.H., Teukolsky, S.A., Vetterling, W.T., Flannery, B.P., 1992. Numerical Recipes. Cambridge University Press, Cambridge.

Van Driel-Gesztelyi, L., Demoulin, P., Mandrini, C.H., 2003. Advances in Space Research 32, 1855–1866.

Zhao, X.P., Hoeksema, J.T., Marubashi, K., 2001. Magnetic clouds Bs events and their dependence on cloud parameters. Journal of Geophysical Research (Space Physics) 106, 15643–15656.